Measuring peripheral wavefront aberrations in subjects with large central visual field loss

L. Lundström*[a], P. Unsbo[a], J. Gustafsson[b]
[a]Biomedical and X-Ray Physics, Royal Institute of Technology, Stockholm, Sweden
[b]Certec, Center of Rehabilitation Engineering Research, Lund University, Sweden

ABSTRACT

Introduction: In a previous study we have shown that correction of peripheral refractive errors can improve the remaining vision in the preferred retinal location (PRL) of subjects with large central visual field loss (CFL). Measuring peripheral refractive errors with traditional methods is often difficult due to the low visual acuity and large aberrations. Therefore a Hartmann-Shack (HS) sensor has been designed to measure peripheral wavefront aberrations in CFL subjects. *Method:* The HS sensor incorporates an eyetracker and analyzing software designed to handle large wavefront aberrations. To ensure that the measurement axis is aligned with the subject's PRL, a special fixation target has been developed. It consists of concentric rings surrounding the aperture of the HS together with a central fixation mark along the measurement axis. *Results:* Some initial measurements on subjects with CFL have been performed successfully. As a first step in improving the peripheral optics of the eye, the wavefront data have been used to calculate the subject's optimal eccentric refraction. *Conclusion:* Measuring the wavefront aberrations is a fast and easy way to assess the details of the optics in subjects with CFL. The wavefront data can then be used to better understand the problems of eccentric correction.

Keywords: peripheral, wavefront aberrations, Hartmann-Shack sensor, central visual field loss, preferred retinal location, eccentric refraction, unwrapping, Zernike polynomials, root mean square (RMS), Strehl ratio

1. INTRODUCTION

Central visual field loss (CFL) is an increasing problem in the ageing population and magnifying devices are currently the only help for affected persons to use their remaining visual function. However, we have recently shown that the remaining vision for these people can be improved by correcting peripheral defocus and astigmatism[1]. The aim of the current work is to evaluate more thoroughly different eccentric corrections by measuring the peripheral wavefront aberrations of individuals with CFL and eccentric fixation.

In an eye with dense or absolute CFL, the fovea is not working and the person has to rely on peripheral vision. Some people with CFL can utilize their remaining vision better by actively using a certain part of the peripheral retina, that is, they are fixating eccentrically to a, so called, preferred retinal location (PRL). The peripheral vision can never fully replace direct or central vision, but with eccentric fixation people with CFL can, to a limited extent, perform visual tasks such as reading or watching television. CFL is the result of a variety of pathologies, like atrophy in the nervus opticus, but the most common cause of CFL is age-related macula degeneration (AMD) and this problem is increasing as the population gets older. It is estimated today[2] that about 8 million people worldwide are severely visually impaired due to macula degeneration. In the U.S. AMD was found to be present in 5% of the population age 65 and older.

Vision in eccentric fixation angles is limited both by the resolution capacity of the peripheral retina and by the large errors (aberrations) in the peripheral optics of the eye. Previously it has been thought that the main limitation is poor retinal capacity and the only help available for CFL patients has been magnifying devices. However, in a previous study we have shown that the remaining vision of subjects with CFL, using a well-defined PRL, can be improved by correcting the peripheral optics[1,3].

Measuring the peripheral optics and refractive errors with traditional methods in subjects with CFL is often difficult due to the large aberrations, reduced retinal function and poor fixation. In the abovementioned study, off-axis refractive errors were measured by photorefraction with the PowerRefractor instrument and a special fixation target was developed to help the subject to hold a stable fixation. Other groups that have investigated peripheral refraction and oblique astigmatism are: Ferree et al., who used a Zeiss parallax optometer[4,5,6]; Millodot, who used a Hartinger optometer[7];

Ophthalmic Technologies XIV, edited by Fabrice Manns, Per G. Söderberg, Arthur Ho, Proceedings of SPIE Vol. 5314 (SPIE, Bellingham, WA, 2004)
1605-7422/04/$15 · doi: 10.1117/12.540885

Rempt et al., who used retinoscopy with the "double sliding-door effect"[8]; and Jennings, Artal, Navarro and Guirao et al., who all used the double-pass method[9,10,11,12,13,14]. However, all of these methods are originally developed for central vision and only give the spherical and cylindrical correction (even though the double-pass method can give an indirect measurement of the higher order aberrations via the point-spread function). In large eccentric fixation angles of 20°-30° off-axis, the oblique astigmatism and higher order aberrations are considerably larger[15]. There is thus a need for methods that give more detailed information about the peripheral optics of the eye. A common way to assess this information is to measure the total wavefront aberrations from the eye with a Hartmann-Shack (HS) sensor. Therefore a laboratory HS sensor has been designed to measure peripheral wavefront aberrations in subjects with CFL and special software has been developed to handle the large aberrations and calculate how the retinal point-spread function (PSF) can be improved. This paper describes the set-up and software and gives example of measurements on a subject with CFL.

2. METHOD

The HS sensor has been designed to measure the eccentric wavefront aberrations of the eye. The principle of the optical set-up resembles a common HS set-up with the pupil of the eye imaged onto a HS sensor (section 2.1.). The set-up incorporates fixation targets to enable subjects with CFL to use eccentric fixation and align the measurement axis with the PRL (section 2.2.). An eyetracker is also built into the system to follow the angle of gaze and the position of the eye (section 2.3.). The raw data from the HS sensor is handled by software specially developed for this purpose (section 2.4.). All measurements on subjects followed the Declaration of Helsinki and were approved by the local Research Ethics Committee. The subjects gave informed consent prior to participation.

The essential components of a HS sensor are a light source, a lenslet array and a CCD-detector[16]. A narrow beam of light is sent into the eye and forms a spot on the retina. Some of the light is reflected and propagates back through the eye as coming from a point source on the retina. The wavefront exiting the pupil contains information about the refractive state and the higher order aberrations of the eye. This wavefront then falls upon the lenslet array of the HS sensor and each lenslet focuses a part of the wavefront onto a CCD-detector in the focal plane of the lenslets (see the inset in figure 1). If the eye is a perfect optical system completely without aberrations, the wavefront out of the eye will be flat. This means that each lenslet will focus its section of the wavefront to a spot right behind the lenslet, to the 'projected lenslet centre'. But if the wavefront is aberrated, its shape will be distorted and the light spots will move away from the projected lenslet centers. The displacement of a spot is proportional to the average tilt of the wavefront over the area of that lenslet. The shape of the wavefront can thus be reconstructed by measuring these displacements.

2.1. Set-up

Figure 1 and the photo in figure 2 show the optics of the HS set-up, which also includes relay lenses imaging the pupil of the eye in the same conjugate plane as the HS sensor. Rail 1 carries the light source, a He-Ne laser (5mW at 633 nm), a shutter controlling the exposure time (typically around 200ms) and optics to collimate the laser light and reduce its intensity. The collimated laser beam finally entering the eye has an intensity of 30μW, which is about one tenth of the safety limits recommended by "The Swedish Radiation Protection Authority"[17]. On rail 2 the aperture (A1) is in a conjugated plane of the pupil and restricts the diameter of the laser beam entering the eye. The glass plate, GP, is used to move the position of the beam entering the pupil. This is necessary to avoid the corneal reflex, which otherwise may disturb the HS image. On rail 3 and 4 two telescopes are mounted, which image the pupil onto the lenslets of the HS sensor. The fast rotating mirror (RM) is used to break the transverse coherence of the laser and avoid speckles in the HS image. The adjustable defocus step (DF) is used to compensate for large amounts of defocus which will blur the HS spots and make them hard to detect. The aperture (A2) limits stray light into the HS sensor, but is large enough to let a highly aberrated wavefront pass. To further reduce stray light rail 3 is partly covered (the cover was removed for the photo in figure 2). The quarter-wave plate (QW), the polarizing beamsplitter (BS) and the polarizer (P) are adjusted to optimize the amount of reflected light from the retina that reaches the lenslets and, at the same time, to minimize the reflexes from the lenses in the set-up. To achieve this, QW makes the vertically polarized laser light circularly polarized. The main part of the reflex from the retina will also be circularly polarized, but in the other rotation direction and after QW it becomes horizontally polarized. It is thus possible to reduce the vertically polarized reflexes from the lenses without damping the faint horizontally polarized light from the eye.

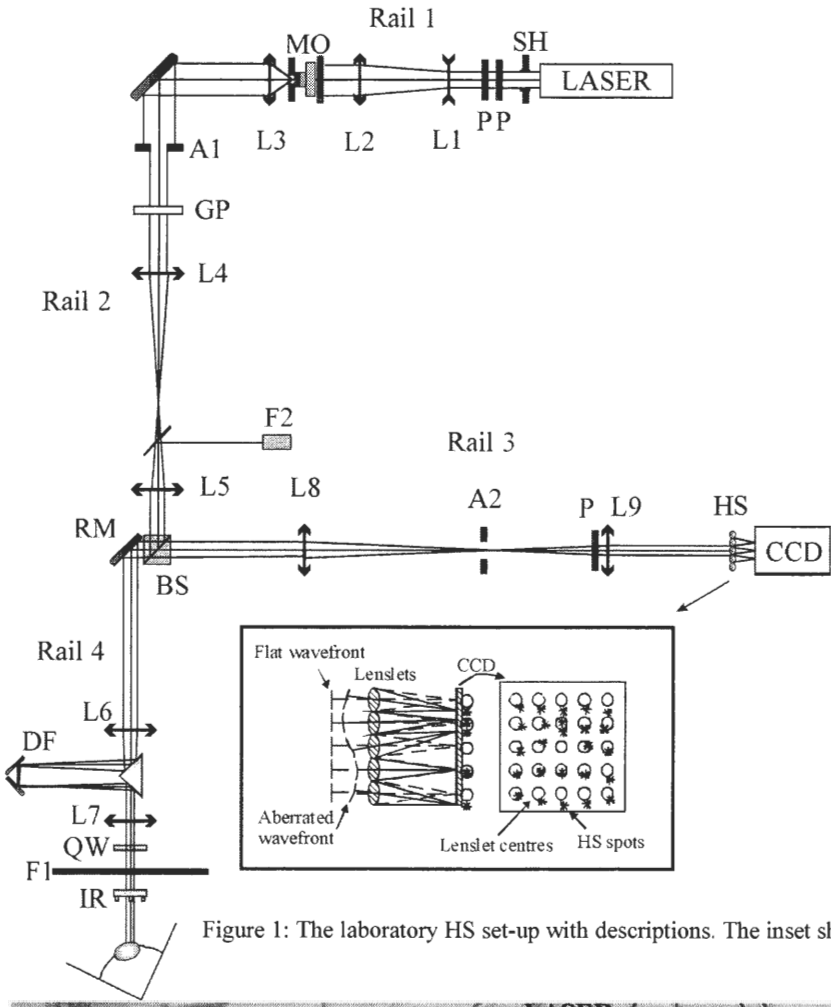

SH = shutter
P = polarizer
L1 = -100 mm
L2 = 200 mm
MO= microscope objective
L3 = 50 mm
A1 = aperture (diam. 2 mm)
GP = glass plate
L4 = 140 mm
F2 = diode fixation target
L5 = 100 mm
BS = polarizing beam splitter
RM= rotating mirror
L6 = 200 mm
DF = defocus step
L7 = 140 mm
QW= quarter wavelength plate
F1 = ring fixation target
IR = IR diodes
L8 = 200 mm
A2 = aperture (diam. 15 mm)
L9 = 140 mm

Figure 1: The laboratory HS set-up with descriptions. The inset shows the principle of the HS sensor.

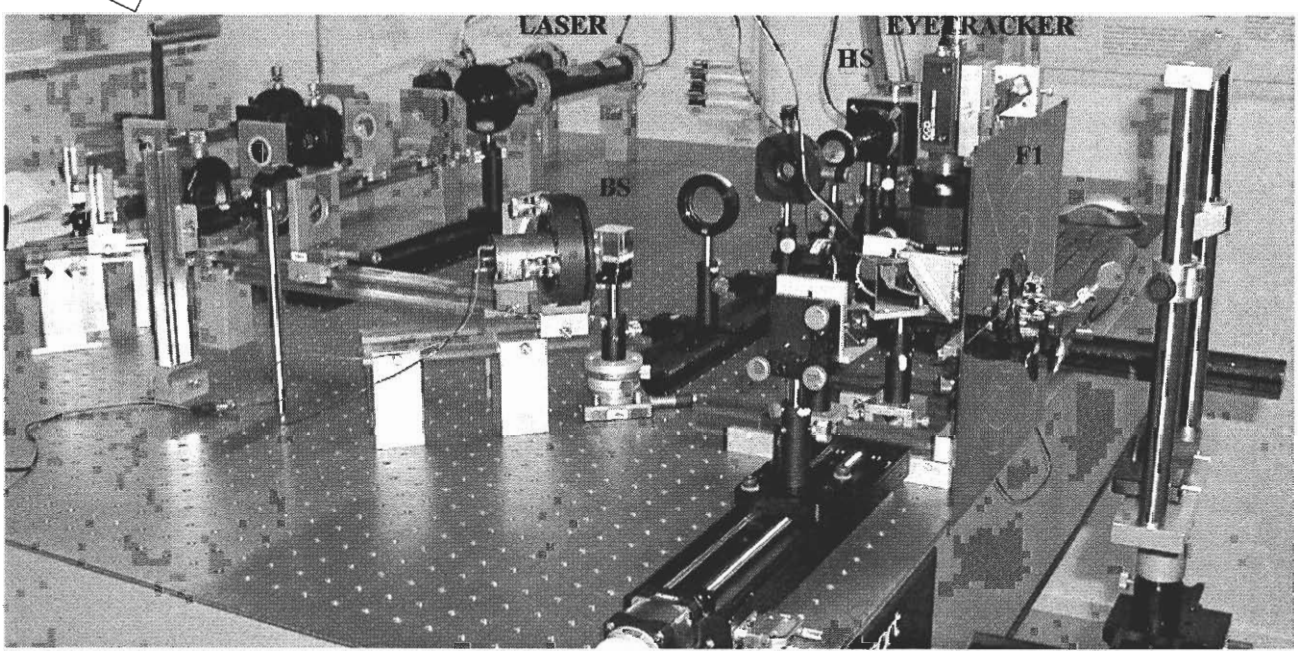

Figure 2: Photo of the HS set-up. Eyetracker camera, ring fixation target, IR diodes and headrest can also be seen.

2.2. Fixation target

When measuring the peripheral wavefront aberrations of an eye with CFL, it is essential that the measurement is performed in the direction that the subject normally uses for vision. That is, the measurement axis of the HS sensor has to be aligned with the subject's PRL. It is also important that the eye does not move, so that the measurement can be repeated. Special fixation targets have therefore been developed to enable the subject to look in the correct direction and keep a stable fixation.

The first fixation target (F1) to be implemented consists of a dark plastic film with multicolored rings surrounding the aperture of L7 and QW in the HS set-up (see figure 3). The film is mounted on an electroluminescent plate which makes the rings appear to glow. The subject will only see the parts of the ring pattern outside his/her scotoma (the dysfunctional region of the retina) and can thus be helped by the rings to place the scotoma in a certain direction and hold it steady (the same principle was used in a previous study[1]). Due to practical reasons the target is placed very close to the eye, about 100mm, which makes it unsuitable for normal, healthy eyes since it stimulates accommodation.

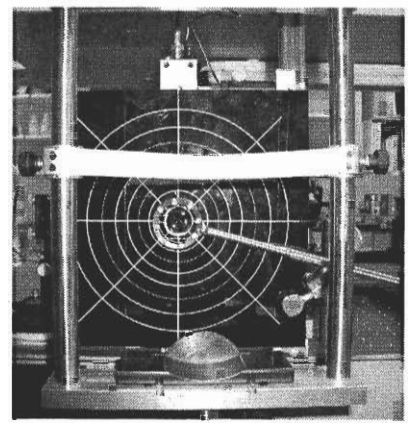

Figure 3: The fixation target with ring patterns seen through the headrest.

The second fixation target (F2) is a green diode aligned with the light path in the HS set-up via a beamsplitter mounted before L5. The diode is aligned with the measurement axis of the HS sensor and should thus be placed in the subject's PRL. That is, the subject should try to direct his/her eye so that the green light is seen as clearly as possible. Since the peripheral retina has limited resolution capacity, this central fixation mark is large and is thus not suitable as a fixation target for normal, healthy eyes.

2.3. Eyetracker

Like most commercial HS sensors this set-up has a pupil camera, which is mounted vertically in between DF and L7. The pupil camera helps the examiner to move the subject's eye to the correct position for the HS sensor. The camera is positioned to have the entrance pupil of the eye in focus and in the middle of the camera image, when the eye is on the axis of and in focus for the HS sensor.

In this set-up the pupil camera has an additional purpose as an eyetracker that tracks the angle of gaze of the eye. The eyetracker software (Tobii Technology Inc®) is specially developed to track an eccentric pupil in real time from the camera images and to save the data of the images, the pupil shape and the angle of gaze. The pupil camera has a filter eliminating visible light to prevent the laser light from disturbing the eyetracker. Instead it uses the illumination from IR diodes, mounted in a ring in between F1 and the eye. To find the direction of the eye, the eyetracker uses the shape of the pupil or the specular reflexes from the IR diodes in the cornea. The angle of gaze data is needed to make sure that the wavefront is measured in the same angle as the subject normally uses and that the direction of the eye remains constant between the measurements.

2.4. Software

After a measurement the HS image has to be computer processed to find the displacements of the spots and to calculate the shape of the wavefront and the PSF. For this purpose we have developed a software package in Matlab® that solves a number of problems associated with measuring the wavefront aberrations in eccentric angles. First of all, the HS image is processed to find the location of the spots (section 2.4.1.). Secondly, the HS spots are correlated with the lenslets they originated from, the so called unwrapping problem (section 2.4.2.). In the third step the shape of the wavefront is reconstructed from the local tilts (section 2.4.3.). Finally, the wavefront aberrations are evaluated to calculate the PSF of the eye and how it is affected by different refractive corrections (section 2.4.4.). The software differs from that of conventional HS sensors especially in how the unwrapping is performed, how the pupil shape is taken into consideration, and how the retinal image is evaluated.

2.4.1. Finding spots

The first part of the software searches for the centers of the spots in the HS image. First of all, the diffuse background is removed. The diffuse background is found by convolving the image with a circle of a diameter of the size of one lenslet. This will spread the intensity in each pixel over a circle and the circles will add up to a slowly varying intensity distribution. This distribution approximately equals the diffuse background and is subtracted from the HS image. Secondly, to reduce the risk of misinterpreting disturbing reflexes as HS spot, the image is low-pass filtered i.e. the high spatial frequencies are removed. The resulting image thus only contains the large structures of the spot pattern. To locate the spots, this filtered image is divided in small squares. The squares are stepped through and a spot is found when the intensity of the brightest pixel in a square exceeds a certain value. Finally, the centroids of the found spots are defined as the centers of gravity in the original image without diffuse background.

2.4.2. Unwrapping

When the centroids of the HS spots have been found the resulting spot pattern must be unwrapped, i.e. for each spot the corresponding lenslet has to be identified. This puts a limit on the measurable shape of a wavefront; if a spot has moved outside the region of its lenslet and closer to another lenslet, it will be harder to assign the spot to the correct lenslet – the so called unwrapping problem. The unwrapping problem occurs when the aberrations are large, e.g. in subjects with a high degree of uncorrected ametropia, keratoconus, penetrating keratoplasty or with central scotomas and eccentric fixation. To solve the unwrapping problem and be able to measure large aberrations, we have developed a software-based unwrapping algorithm[18]. An alternative to a software algorithm is to use hardware solutions, e.g. lenslets with a lower f-number, optics to compensate for defocus and astigmatism, a moveable aperture transmitting the spot from only one lenslet at a time[19], or astigmatic lenslets for easier identification of the spots[20]. But a well designed software algorithm has the advantage over hardware methods that it can handle wavefront aberrations from highly aberrated eyes without reducing the accuracy or introducing a higher complexity into the optics of the HS set-up.

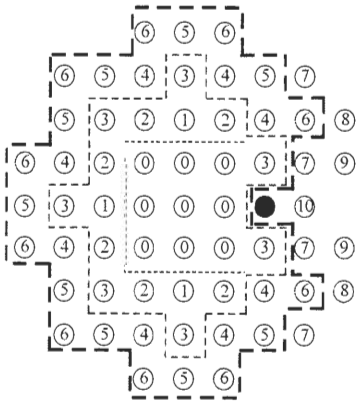

Figure 4: The progression of the iteration. 0 = starting lenslets, 1 = lenslets connected in the first iteration, 2 = lenslets connected in the second iteration etc. The filled circle represents a lenslet without a HS spot.

The algorithm we have developed starts by connecting the central 3×3 HS spots with the closest projected lenslet centers. From these connected pairs the locations of the HS spots, corresponding to the other lenslets, are predicted. The prediction is performed by least squares fitting a B-spline function to the displacements of the connected HS spots[18,21]. This function is then extrapolated outwards, to the closest not-yet-connected lenslets, to give expected locations of their HS spots. A new HS spot will be connected if it lies close enough to one of these expected locations. The algorithm continues in an iterative manner and ends when no more pairs can be connected.

This gradual iteration with fitting, extrapolating, connecting and fitting again, means that the algorithm will iterate outwards in circles as shown in figure 4. If a HS spot is missing or too far away from the predicted location, the corresponding lenslet will be left unconnected in that iteration, but will be rechecked in each of the following iterations until it is connected or all HS spots are identified. Thus, this technique enables the algorithm to work around difficult parts in the HS spot pattern and to handle missing HS spots (an example of this is seen in figure 4).

2.4.3. Wavefront reconstruction

The algorithm for wavefront reconstruction uses the measured HS spots and spots originating from a reference wavefront without any aberrations. The reference image is obtained by sending a flat wavefront into the HS set-up from the position of the eye. The local tilts T_x and T_y, in the x and y direction, of the wavefront are found from the distances between the HS spots and the reference spots, divided by the focal length of the lenslets. The tilts are measurements of the partial derivatives of the wavefront and should thus be integrated. This algorithm, like most other HS systems, uses Zernike polynomials to reconstruct the wavefront. The Zernike polynomials, Z_n^m, (where n is the radial order and m is the azimuthal frequency[22]) constitute a complete, orthogonal set of polynomials defined over a unit circle. Thus, any physical wavefront Φ can be expanded into Zernike polynomials:

$$\Phi(x,y) = \sum_{n,m} c_n^m Z_n^m(x,y),$$

where c_n^m are the Zernike coefficients (in microns) and (x, y) are normalized coordinates in the pupil plane. Each Zernike polynomial describes a certain aberration and the coefficient gives the amount of that aberration in the current wavefront. The second order (n=2) terms, for example, correspond to astigmatism and defocus, other, higher order terms are similar to the familiar Seidel aberrations coma and spherical aberration etc.

To reconstruct the wavefront, the Zernike coefficients are found by a least squares fit of the partial derivatives of the wavefront to the measured local tilts according to:

$$T_x(x_p,y_p) = \sum_{n,m}(c_n^m / r_{pupil})\frac{\partial Z_j(x_p,y_p)}{\partial x}$$

$$T_y(x_p,y_p) = \sum_{n,m}(c_n^m / r_{pupil})\frac{\partial Z_j(x_p,y_p)}{\partial y},$$

where (x_p, y_p) are the positions of the individual lenslets in the pupil plane (sampling points) and r_{pupil} is the radius of the pupil in microns[23].

When eccentric wavefront aberrations are reconstructed, a complication arises since the pupil is not circular. In oblique angles the pupil and the wavefront leaving it will be elliptic, but the Zernike polynomials are defined over a circle. We have solved this by reconstructing the wavefront over a circle with a radius equal to the major axis of the elliptic pupil. There will thus be an extrapolated part of the wavefront outside the pupil that has no physical relevance. When the aberrations are evaluated, this part should be cut away.

To minimize the influence of fluctuations in the higher order aberrations, due to the tear film etc., multiple measurements are made. The Zernike coefficients are calculated for each measurement and are then averaged to describe the total wavefront. It is thus very important to measure in the same angle each time and the eyetracker gives a good measure of whether two measurements can be averaged or not.

2.4.4. Correction evaluation

The Zernike coefficients are a measure of the wavefront aberrations in the optics of the eye, and with the help of them different optical corrections can be evaluated. The optimum correction would of course be to correct all aberrations so that the wavefront is completely flat. This is unfortunately impossible except in an adaptive optics system. The aim is thus to give the subject as good vision as possible with available means. Most common in an optometrist's practice is to use spherical and cylindrical correction with spectacles or contact lenses. An important problem is to know what "as good vision as possible" means and thus by which metric to optimize. The metrics available are usually divided into two groups: pupil plane metrics, based directly on the wavefront aberrations, and image plane metrics, where the wavefront aberrations are computed further to calculate the retinal image. According to Guirao and Williams[24] the image plane metrics corresponds well with subjective impressions for normal foveal vision, while the pupil plane metrics give a poor prediction, especially when the aberrations are large.

We calculate the optimum spherical and cylindrical correction by two methods; a pupil plane metric method which minimizes the root mean square (RMS) of the wavefront error, and an image plane metric method which calculates the PSF of the retinal image and optimizes the Strehl ratio.

The pupil method with minimum RMS is currently often used to find the optimum correction centrally. It means that the refractive correction simply can be calculated from the second order Zernike coefficients c^{-2}_2, c^0_2, c^2_2:

$$M = -\frac{4\sqrt{3}}{r_{pupil}^2}c_2^0 \qquad C_{0°} = \frac{4\sqrt{6}}{r_{pupil}^2}c_2^2 \qquad C_{45°} = \frac{4\sqrt{6}}{r_{pupil}^2}c_2^{-2}$$

where the coefficients and the radius of the pupil, r_{pupil}, are in microns. In the equations above the refractive correction is expressed as an astigmatic decomposition[25] with mean sphere, M, one cylinder component with axis 0°, $C_{0°}$, and one cylinder component with axis 45°, $C_{45°}$. These can be translated into traditional sphere, cylinder, and axis in the following manner:

$$\text{cylinder} = -\sqrt{C_{0°}{}^2 + C_{45°}{}^2}$$

$$\text{axis} = \arctan\left(\frac{\text{cylinder} - C_{0°}}{C_{45°}}\right)$$

$$\text{sphere} = M - \frac{\text{cylinder}}{2}$$

The image plane method uses the PSF which describes the retinal image of a point-like object. The PSF is found by Fourier transformation of the generalized pupil function, $\boldsymbol{P}(x,y)$[26]:

$$\text{PSF} = \frac{\left|\Im\{\boldsymbol{P}(x,y)\}\right|^2}{\text{pupil area}}$$

$$\boldsymbol{P}(x,y) = \text{P}(x,y)\cdot e^{-i\frac{2\pi}{\lambda}WFA(x,y)}$$

where x and y are the coordinates in the pupil. The generalized pupil function includes the height of the measured wavefront, WFA(x,y), and the shape of the pupil, P(x,y), which equals one inside the pupil and zero outside. We thus take the elliptic shape of the pupil into consideration with this calculation, since only the wavefront inside the pupil is used for computing the PSF. The pupil shape can be taken from either the eyetracker or the HS image. The peak value of the PSF, the Strehl ratio, is then optimized by trial and error. A wide range of combinations of spherical and cylindrical values are stepped through and the Strehl ratio for each combination is computed. The sphere and cylinder values are chosen ±10D in 0.1D step around the values which give the minimum RMS-value of the wavefront. The combination that gives the largest Strehl ratio is regarded as the optimum one. This method is not limited to spherical and cylindrical values; it can also be used to optimize various aberration corrections.

3. RESULTS

The HS sensor and the software have been tested successfully in eccentric fixation angles on a number of subjects with CFL. The subjects have found the fixation targets to be a useful help to align their PRL with the measurement axis of the sensor and to keep their fixation stable. It was thus possible to make multiple measurements in the PRL of each subject. The quality of the HS images is good, without disturbing reflexes and stray light, and the wavefronts have been successfully unwrapped and reconstructed. The measured aberrations and the pupil sizes have been used to find optimal spherical and cylindrical corrections by minimizing the RMS and by optimizing the Strehl ratio. As an example the measurements from one subject is presented.

The subject is a woman born 1943, who has suffered from AMD many years and has a large CFL with a radius of about 20°. Her right eye has a well trained PRL 22° nasally. Five measurements in her PRL has been preformed in a dark room with her normal pupil size (no cycloplegia was used). Only the ring pattern fixation target was in use when she was measured, since the central diode fixation target was not yet implemented. She commented that it was much easier to keep the eye stable with the fixation target than without. Table 1 shows that her fixation was stable during all five measurements, which were all taken within a few minutes.

The results from the measurements are presented in figure 5. The first three images show the eyetracker image (a), the original HS image (b) and the unwrapped HS spot pattern (c) for the first measurement. Figure 5d is the wavefront reconstructed from the average Zernike coefficients of all five measurements.

Measurement	1	2	3	4	5
φ	349°	346°	339°	358°	353°
θ	22°	22°	20°	23°	23°

Table 1: The subject's angle of fixation for each measurement. φ is the direction angle (0°=left, 90°=up etc.) and θ is the radial angle (0°=the central visual axis of the eye is aligned with the HS axis).

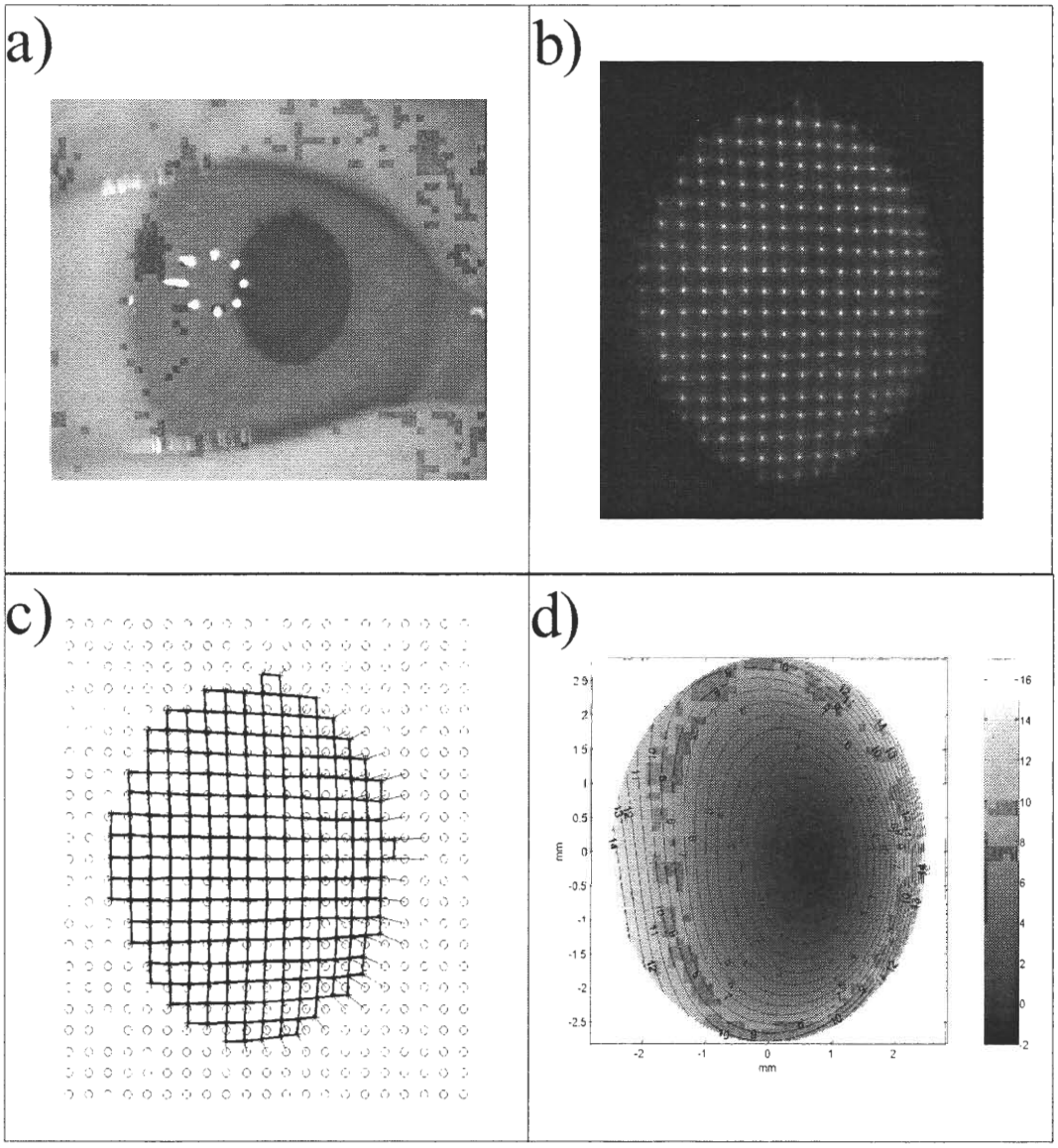

Figure 5: Example showing (a) the image from the eyetracker and (b) the original HS image. In (c) the spot pattern is unwrapped and each HS spot (star) is connected to its corresponding lenslet (circle). In (d) the wavefront is reconstructed from the average of five separate measurements.

The optimum spherical and cylindrical refraction was -2.5 DS, -2.5 DC axis 98° with the minimum RMS method and +0.5 DS, -1.25 DC axis 151° with the maximum Strehl method. For comparison, the PSF and the retinal image of a Snellen letter chart have been simulated in figure 6, with no correction, with RMS correction, and with Strehl correction. As can be seen from the shape of the uncorrected PSF, coma and oblique astigmatism are large in this oblique angle. With correction, the contrast in the retinal image of the chart is severely lowered by the remaining coma.

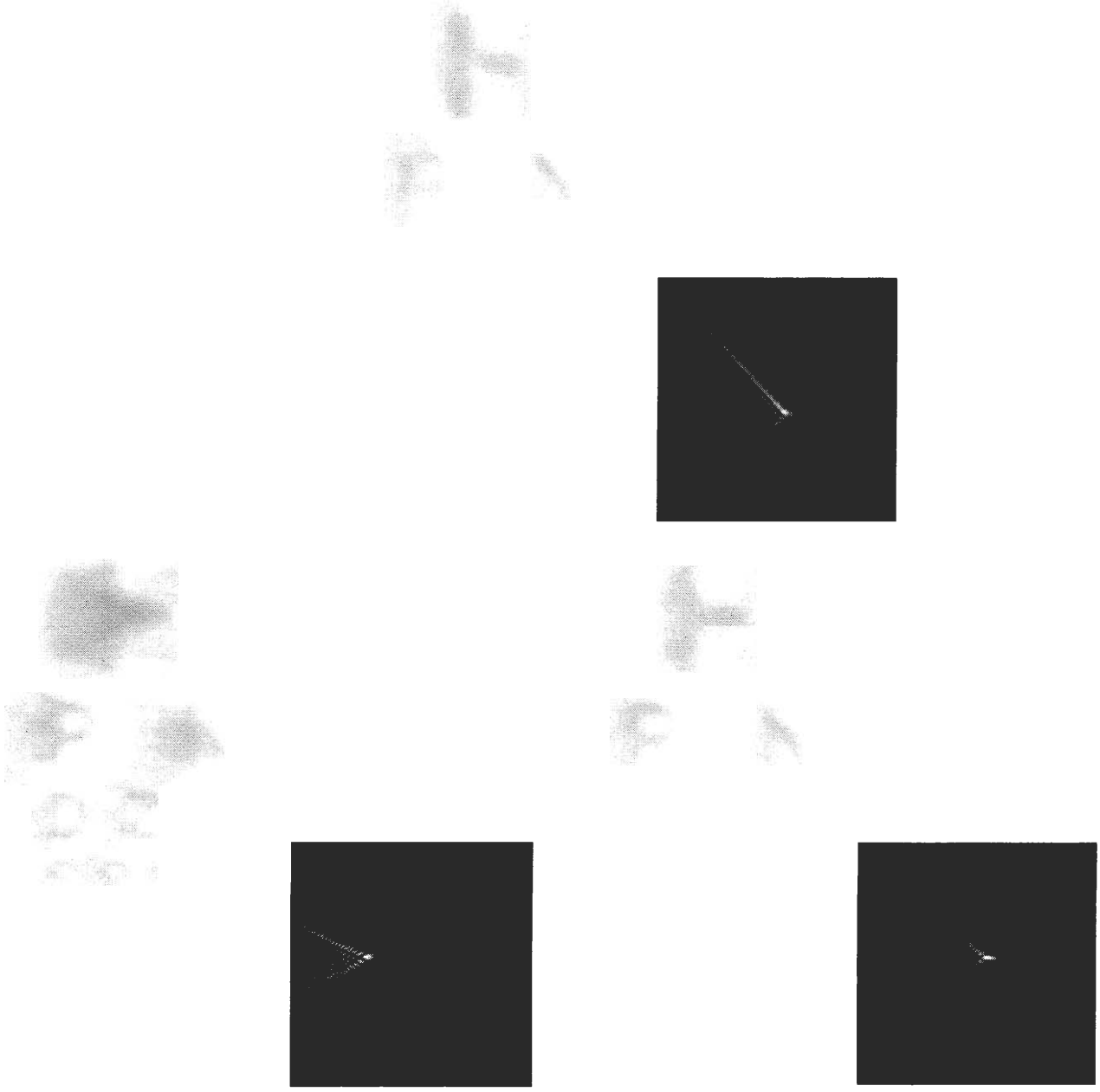

Figure 6: Simulation of the retinal image of a letter chart and a point spread function in the subject's PRL without correction (upper), with RMS correction -2.5 DS, -2.5 DC axis 98°(lower left), and with Strehl correction +0.5 DS, -1.25 DC axis 151°(lower right).

4. SUMMARY AND DISCUSSION

We have recently shown that the remaining vision of subjects with CFL can be improved by correcting the peripheral optics of the eye. The reason for why peripheral correction has not previously been used is that the eccentric vision was thought to be limited by the retinal resolution. The peripheral optics of the eye often suffers from large aberrations, and this together with the low visual acuity makes it very difficult to assess the required correction with subjective methods

for central vision. The technique we have developed measures the wavefront aberrations in the subject's PRL with an objective HS sensor designed for peripheral measurements. A software package reconstructs the largely aberrated wavefront, expressed in Zernike polynomials, with the help of a special unwrapping algorithm. The technique thus gives a detailed description of the optics in the subject's PRL. This information can then be used to evaluate the effect of different corrections.

Two methods are used to optimize the spherical and cylindrical correction; minimizing the RMS and optimizing the Strehl ratio. The main difference between these is that the RMS method only uses the second order aberration terms, while the Strehl method takes all aberrations into consideration. The higher order aberrations contain components resembling defocus and astigmatism and will thus affect the optimum spherical and cylindrical correction, especially when the aberrations are large. Therefore, we prefer to use the Strehl method in peripheral measurements. Another advantage with the Strehl method and the trial and error process is that it will not be mislead by, what optics designers call, local minima. A local minimum for a certain correction means that the retinal image quality is better here compared to what it is for other, slightly different corrections. But if the correction is changed more radically, another minimum can be found with even better image quality. In the peripheral optics of the eye, the higher order aberrations increase the risk of being trapped in a local minimum. The trial and error technique avoids this by objectively comparing a wide range of corrections. The simulations in figure 6 also show the effect of local minima. The large difference between the two corrections (-2.5 DS, -2.5 DC axis 98° and +0.5 DS, -1.25 DC axis 151°) would give larger difference in image quality for central vision, but in the subject's PRL the large aberrations can give rise to a number of local minima.

Maximizing the Strehl ratio is not the only metric that can be used. Other retinal image plane metrics, as for example the width of the PSF, may also be useful. Mouroulis et al.[27] claim that the maximum Strehl ratio might be misleading if the aberrations are very large and the Strehl ratio is very low. However, in the future the choice of image plane metric would probably be a minor problem if, e.g., contact lenses can be specially designed to compensate higher order aberrations. The PSFs in figure 6 show that coma correction would improve the retinal image quality considerably.

As a first step the CFL subjects have been prescribed spherical and cylindrical correction of the optical errors in their PRL based on wavefront measurements. Currently the improvement in visual function is evaluated. A study is also preformed to compare the eccentric refractive errors measured by the HS sensor with other refraction methods. A future development is to try to correct coma.

ACKNOWLEDGMENTS

The financial support for this research, provided by the Göran Gustafsson Foundation, the Carl Trygger Foundation and the Carl-Johan and Berit Wettergren Foundation, is greatly appreciated.

REFERENCES

1. J.Gustafsson and P.Unsbo, "Eccentric Correction for Off-Axis Vision in Central Visual Field Loss," Optom.Vis.Sci. **7**, 535-541 (2003)
2. R.Leonard, "Statistics on Vision Impairment: A Resource Manual," Arlene R. Gordon Research Institute of Lighthouse International, 5th edition (2002)
3. J.Gustafsson, "The first successful eccentric correction," Visual Impairment Research **3**, 147-155 (2002)
4. C.E.Ferree, G.Rand, and C.Hardy, "Refraction for the peripheral field of vision," Archives of Ophthalmology **5**, 717-731 (1931)
5. C.E.Ferree, G.Rand, and C.Hardy, "Refractive asymmetry in the temporal and nasal halves of the visual field," Am.J.Ophthalmol. **15**, 513-522 (1932)
6. C.E.Ferree and G.Rand, "Interpretation of refractive conditions in the perpheral field of vision," Archives of Ophthalmology **9**, 925-938 (1933)
7. M.Millodot, "Effect of Ametropia on Peripheral Refraction," American Journal of Optometry & Physiological Optics **58**, 691-695 (1981)

8. F.Rempt, J.Hoogerheide, and W.P.H.Hoogenboom, "Peripheral Retinoscopy and the Skiagram," Ophthalmologica **162**, 1-10 (1971)
9. J.A.M.Jennings and W.N.Charman, "Optical Image Quality in the Peripheral Retina," American Journal of Optometry & Physiological Optics **55**, 582-590 (1978)
10. J.A.M.Jennings and W.N.Charman, "Off-Axis Image Quality in the Human-Eye," Vision Research **21**, 445-455 (1981)
11. R.Navarro, P.Artal, and D.R.Williams, "Modulation Transfer of the Human Eye as a Function of Retinal Eccentricity," J.Opt.Soc.Am.A **10**, 201-212 (1993)
12. P.Artal, A.M.Derrington, and E.Colombo, "Refraction, Aliasing, and the Absence of Motion Reversals in Peripheral Vision," Vision Research **35**, 939-947 (1995)
13. J.A.M.Jennings and W.N.Charman, "Analytical Approximation of the Off-axis Modulation Transfer Function of the Eye," Vision Research **37**, 697-704 (1997)
14. A.Guirao and P.Artal, "Off-axis monochromatic aberrations estimated from double pass measurements in the human eye," Vision Research **39**, 207-217 (1999)
15. J.Gustafsson, E.Terenius, J.Buchheister, and P.Unsbo, "Peripheral astigmatism in emmetropic eyes," Ophthalmic Physiol. Opt. **21**, 393-400 (2001)
16. J.Liang, B.Grimm, S.Goelz, and J.F.Bille, "Objective measurement of wave aberrations of the human eye with the use of a Hartmann-Shack wave-front sensor," J.Opt.Soc.Am.A **11**, 1949-1957 (1994)
17. *The Swedish Radiation Protection Institute's Regulations on Lasers*, SSI FS 1993:1 (1993)
18. L.Lundström and P.Unsbo, "Unwrapping Hartmann-Shack Images from Highly Aberrated Eyes Using an Iterative B-Spline Based Extrapolation Method," accepted for publication in Optom.Vis.Sci. (2004)
19. S.Olivier, V.Laude, and J.P.Huignard, "Liquid-crystal Hartmann wave-front scanner," Applied Optics **39**, 3838-3846 (2000)
20. N.Lindlein and J.Pfund, "Experimental results for expanding the dynamic range of a Shack-Hartmann sensor using astigmatic microlenses," Opt.Eng. **41**, 529-533 (2002)
21. S.Groening, B.Sick, K.Donner, J.Pfund, N.Lindlein, and J.Schwider, "Wave-front reconstruction with a Shack-Hartmann sensor with an iterative spline fitting method," Applied Optics **39**, 561-567 (2000)
22. L.N.Thibos, R.A.Applegate, J.Schwiegerling, R.Webb, and VISA Standards Taskforce Members, "Standards for Reporting the Optical Aberrations of Eyes," Trends in Optics and Photonics **35** (2000)
23. R.Cubalchini, "Modal wave-front estimation from phase derivative measurements," J.Opt.Soc.Am. **69**, 972-977 (1979)
24. A.Guirao and D.R.Williams, "A method to predict refractive errors from wave aberration data," Optom.Vis.Sci. **80**, 36-42 (2003)
25. R.B.Rabbetts, *Bennett & Rabbetts' Clinical Visual Optics*, Butterworth-Heinemann, 3rd edition (1998)
26. J.W.Goodman, "Frequency Analysis of Optical Imaging Systems," Ch. 6, 126-71, in *Introduction to Fourier optics,* The McGraw-Hill Companies Inc., 2nd edition (1996)
27. P.Mouroulis and H.Zhang, "Visual instrument image quality metrics and the effects of coma and astigmatism," J.Opt.Soc.Am.A **9**, 34-42 (1992)

*linda@biox.kth.se; phone +46 (0)8 55 37 81 24; www.biox.kth.se/visual_optics/